scientific reports

Check for updates

OPEN

YTHDF2 promotes the metastasis of oral squamous cell carcinoma through the JAK-STAT pathway

Zhezheng Chen[1,2,3,5], Dan Zhao[1,2,5], Yamin Yuan[2], Lu Zeng[2,4], Zhengzhou Luo[1,2,3], Junliang Chen[1,2,3], Xiaorong Lan[2], Yun He[1,2,3]✉ & Lin Liu[1,2,3]✉

RNA-binding proteins act as crucial mediators between N6-methyladenosine (m6A) modification and RNA function, playing a significant role in the recurrence and metastasis of oral squamous cell carcinoma (OSCC). YTHDF2, the first identified RNA-binding protein, has been shown to be closely associated with the prognosis of certain types of cancer. However, the role of YTHDF2 in OSCC and its underlying molecular mechanisms remain poorly understood and require further investigation. First, we analysed the expression levels of YTHDF2 and examined its correlation with clinical features using public databases and OSCC patient samples. Subsequently, a series of in vitro functional experiments were conducted to assess the effects of YTHDF2 on the proliferation, migration, and invasion capabilities of OSCC cells. Additionally, RNA-seq analysis was utilized to investigate the signalling pathways modulated by YTHDF2, which was further supported by experimental validation. Our findings revealed that YTHDF2 expression was significantly elevated in OSCC tissues and cells, with levels closely correlated with the clinical stage, pathological grade, and survival time of patients. The knockdown of YTHDF2 resulted in a significant reduction in the proliferation, migration, and invasion abilities of OSCC cells. Furthermore, RNA sequencing data indicated that silencing YTHDF2 suppressed the JAK-STAT signalling pathway, and the use of STAT3 activators reversed this suppressive effect in OSCC cells. Our study demonstrated that YTHDF2 promotes the proliferation, metastasis, and invasion of OSCC by positively regulating the JAK-STAT signalling pathway, suggesting that YTHDF2 could serve as a potential prognostic marker for the diagnosis and treatment of OSCC.

Keywords YTHDF2, Oral squamous cell carcinoma, Metastasis, JAK-STAT pathway, m6A

Oral squamous cell carcinoma (OSCC) is one of the most common oral cancers worldwide and is often linked to smoking, alcohol consumption, and human papillomavirus infection[1]. Globally, OSCC accounts for more than 90% of oral malignancies, with over 500,000 new cases and 170,000 fatalities reported annually, with increasing incidence. It is expected that by 2030, the annual incidence rate of OSCC will increase to 30%, resulting in 1.08 million new cases[2]. Unfortunately, the early diagnosis rate of OSCC is low and often coincides with lymph node metastasis. Approximately 70% of patients are diagnosed at an advanced stage, with significant lymph node metastasis; this results in an approximate 50% decrease in the 5-year survival rate[3]. The primary reason for this situation is that the main factors contributing to the poor therapeutic effects on OSCC—local recurrence and distant metastasis—have not been effectively resolved[4]. Therefore, understanding the molecular mechanisms underlying OSCC recurrence and metastasis as well as finding new therapeutic targets are crucial areas of current research.

During the process of OSCC metastasis, cells develop the ability to metastasize through genetic or epigenetic changes. Among these changes, epigenetic modifications at the RNA level, particularly 6-methyladenine (N6-methyladenosing, m6A), have garnered significant attention[5]. m6A is the most common RNA modification in eukaryotes, and its addition and removal are dynamic and reversible processes[6]. This process is regulated by methyltransferases, which add m6A; demethylases, which remove m6A; and m6A-binding proteins[6]. These m6A-binding proteins serve as critical mediators by linking m6A modifications to RNA function. Specific target

[1]Department of Oral and Maxillofacial Surgery, The Affiliated Stomatological Hospital of Southwest Medical University, Luzhou 646000, China. [2]Luzhou Key Laboratory of Oral and Maxillofacial Reconstruction and Regeneration, Luzhou 646000, China. [3]Department of Oral and Maxillofacial Surgery, The Affiliated Hospital of Southwest Medical University, Luzhou 646000, China. [4]Department of Oral Implantology, The Affiliated Stomatological Hospital of Southwest Medical University, Luzhou 646000, China. [5]Zhezheng Chen and Dan Zhao contributed equally to this work. ✉email: heyundaidai@163.com; drliulin@163.com

genes of m6A modification regulate the splicing, processing, transport, translation, and stability of RNA, thereby impacting the proliferation, migration, invasion, and chemotherapy resistance of tumour cells[7]

Notably, YTHDF2, identified as the first and most effective m6A reading protein, has been found to have dual functions in regulating the proliferation and migration of tumour cells[8]. For instance, YTHDF2 was shown to promote tumor progression in acute myeloid leukaemia, lung cancer, and bladder cancer by stabilizing oncogenic mRNAs, thereby enhancing cancer cell proliferation and metastasis[9,10,11]. In contrast, YTHDF2 exerts tumor-suppressive effects in gastric cancer and melanoma by destabilizing oncogenic mRNAs, indicating that its function is highly context-dependent and tumor-type specific[12,13]. Nevertheless, there is little research on the role of YTHDF2 in OSCC.

The JAK-STAT signaling pathway regulates cell proliferation, differentiation and immune responses, playing a crucial role in the progression of cancer, particularly in OSCC. For example, the interaction between PD-L1 and the JAK2-STAT3/MAPK-AP1 pathway has been reported to promote cancer progression, invasion, and therapy resistance[14]. Furthermore, a recent study using bioinformatics analysis identified YTHDF2, along with other m6A methylation regulators, as a critical gene in OSCC progression[15]. Specifically, silencing YTHDF2 suppressed this pathway, leading to decreased proliferation, migration, and invasion abilities in OSCC cells. Additionly, the use of STAT3 activators reversed these suppressive effects, indicating that YTHDF2 may exert its oncogenic role through modulation of the JAK-STAT pathway. These findings underscore the importance of the JAK-STAT signaling pathway in OSCC progression and suggest that YTHDF2 may serve as a potential prognostic biomarker and therapeutic target in OSCC. Further research is warranted to explore the precise mechanisms underlying the interaction between YTHDF2 and the JAK-STAT pathway in OSCC and other cancers.

This study analysed the expression of YTHDF2 in OSCC tissues compared with that in control tissues, as well as the relationships between YTHDF2 levels and the clinical characteristics and survival times of OSCC patients. Functional experiments were conducted to elucidate the regulatory effect of YTHDF2 on OSCC proliferation and metastasis. Additionally, transcriptome sequencing was performed to identify the signalling pathways through which YTHDF2 regulates the biological behaviour of OSCC cells. Our research particularly focused on the interaction between YTHDF2 and the JAK-STAT signaling pathway as a critical mechanism in mediating its oncogenic effects. Overall, this research provides insights into the molecular mechanisms underlying YTHDF2-mediated proliferation and metastasis in OSCC, suggesting a potential therapeutic target for future studies.

Materials and methods

Clinical samples

The study analysed a group of 59 squamous cell carcinoma tissue samples and 20 paracancerous tissue samples from patients treated at the Department of Oral and Maxillofacial Surgery, Stomatological Hospital Affiliated with Southwest Medical University, between January 2018 and December 2020. The follow-up deadline was January 2024. None of the patients had undergone preoperative radiation or chemotherapy, and all tissue samples were obtained with appropriate informed consent and approval from the Institutional Review Board of the Stomatological Hospital Affiliated with Southwest Medical University. We confirm that all experiments were performed in accordance with relevant guidelines and regulations.

IHC staining

All the tissue sections were deparaffinized, rehydrated, subjected to antigen retrieval, blocked and incubated with an anti-YTHDF2 antibody (1:2000, Abcam) overnight at 4 °C. This was followed by incubation with secondary antibodies and detection via a diaminobenzidine (DAB) kit (Gene Tech, China), followed by haematoxylin counterstaining. The images were captured via an upright microscope system (Nikon, Japan), and the YTHDF2 immunostaining score was calculated by multiplying the score for the proportion of positively stained tumour cells (categories: 1 (< 25%), 2 (25–50%), 3 (50–75%), and 4 (> 75%) by the score for staining intensity (categories: 1-weak staining, 2-moderate staining, and 3-strong staining). The staining score was assessed by two blinded pathologists, and patients were categorized into low-staining (1–6) and high-staining (8–12) groups. Detailed patient information can be found in Table S1.

Cell culture and transfection

SCC9 and NOK (normal oral keratinocytes) cells were kindly provided by Professor Wang[15]. SCC9 is a widely used human tongue squamous cell carcinoma cell line, chosen for its relevance in OSCC research due to its well-characterized genetic and phenotypic properties. NOK was selected as a control to represent normal oral mucosal cells. SCC9 cells were cultured in DMEM/F12 (Gibco, USA), and NOK cells were cultured in high-glucose DMEM (Gibco, USA). The SCC9 culture medium was supplemented with 10% foetal bovine serum (FBS, Gibco, USA), 1% penicillin–streptomycin (Beyotime Biotech, China), and 400 ng/mL hydrocortisone (Sigma, USA), which is essential for supporting the specific growth requirements of SCC9 cells. NOK cell culture medium contained 10% FBS and 1% penicillin–streptomycin. Both cell lines were maintained in a humidified incubator at 37 °C with 5% CO_2. The culture medium was refreshed every 2–3 days. Subculturing was performed when the cells reached approximately 80% confluence, and cell viability was routinely checked to ensure reproducibility.

Plasmid transfection was conducted via a siRNA transfection kit (Ribo, China) following the manufacturer's instructions, with three YTHDF2 siRNA sequences designed: siYTHDF2-1, GACCAAGAATGGCATTGCA; siYTHDF2-2, GCACAGAAGTTGCAAGCAA; and siYTHDF2-3, GGTAGCGGGTCCATTACTA.

Quantitative real-time PCR (qRT–PCR)

Total RNA was extracted from cells via the Steady Pure Rapid RNA Extraction Kit according to the manufacturer's instructions. The RNA concentration and purity were measured using a NanoDrop 2000 spectrophotometer

(Thermo Fisher Scientific). RNA samples with an A260/A280 ratio of 1.8–2.0 were used for subsequent experiments. This was followed by cDNA synthesis with ReverTra Ace qPCR RT Master Mix (Toyobo, Japan). PCR was then conducted via the SYBR Green Master Mix Kit (Takara, Japan) on a StepOne Plus Real-time PCR System (Applied Biosystems, USA), with GAPDH as the internal control. The reaction system included 10 μL SYBR Green Master Mix, 1 μL cDNA template, 0.4 μL of forward and reverse primers (10 μM each), and 8.2 μL nuclease-free water, resulting in a total reaction volume of 20 μL.

The thermal cycling conditions were as follows: initial denaturation at 95 °C for 30 s, followed by 40 cycles of denaturation at 95 °C for 5 s and annealing/extension at 60 °C for 30 s. Each sample was analysed in triplicate, with data analysis based on the $2^{-\Delta\Delta CT}$ method. The primers used are listed in Table S2.

Western blot

Cellular proteins were extracted by lysing cells in RIPA buffer supplemented with protease inhibitors (Sigmar, USA). The extracted protein concentrations were detected via a BCA kit. Subsequently, 20 μg of protein per sample was separated via 10% sodium dodecyl sulfate–polyacrylamide gel electrophoresis (SDS-PAGE) and transferred onto a PVDF membrane (Millipore, USA). The samples were incubated overnight at 4 °C with primary antibodies against YTHDF2 (1:1000, Abcam, catalog # ab220163), JAK2 (1:5000, Abcam, catalog # ab108596), STAT3 (1:1000, Abcam, catalog # ab68153), p-JAK2 (1:5000, Abcam, catalog # ab32101), p-STAT3 (1:1000, Abcam, catalog # ab76315), and GAPDH (1:10000, Affinity Biosciences, catalog # AF7021). The membranes were then washed three times with TBST buffer (Tris-buffered saline containing 0.1% Tween 20) for 5 min each.

The samples were incubated with an HRP-labelled secondary antibody (1:1000, Beyotime, catalog # A0208) for 1 h at room temperature. The membranes were washed again three times with TBST buffer for 5 min each. Protein bands were detected using an enhanced chemiluminescence kit (Thermo Fisher Scientific, catalog # 32106) and visualized with the ChemiDoc Imaging System (Bio-Rad). Signal intensity was quantified using Image Lab software (Bio-Rad).

Proliferative assay

Cell proliferation was assessed through CCK-8 and colony formation assays. For the CCK-8 assay, cells were plated in 96-well plates at a density of 2000 cells per well. The absorbance was measured at 0, 24, 48, 72, and 96 h at a wavelength of 450 nm postseeding via the CCK-8 system (Dojindo, Japan). For the colony formation assay, cells were seeded in 6-well plates at a density of 1000 cells per well and cultured in DMEM/F12 medium supplemented with 10% FBS for approximately 2 weeks. Colonies were visualized and quantified after fixation with methanol and 0.1% crystal violet staining for 30 min.

Scratch wound assay

The cells were seeded into 6-well plates and allowed to grow until they reached confluence. A scratch of approximately 1 mm in the confluent cell layer was made via a P200 pipette tip, followed by continued cell culture. Images were captured at 0, 24, 48, and 72 h, and the reduction in the wound area was analysed via ImageJ software.

Cell migration and invasion assays

Cell migration and invasion abilities were assessed using chambers with or without Matrigel. A cell suspension was prepared in serum-free DMEM/F12 medium at a concentration of 1×10^5; 500 μL of the suspension was placed in the upper chamber; and 1 ml of DMEM/F12 medium containing 10% FBS was added to the lower chamber. After incubation for 24 h, the cells on the upper surface of the filter were removed, and those that had migrated through the filter and adhered to the lower surface were stained with 0.1% crustal violet. Five random fields of view were selected under a microscope, images were captured, and the cells were quantified.

Transcriptome sequencing

Total RNA was extracted from three groups of SCC9 cells transfected with siYTHDF2 or control plasmid and sent to Lianchuan Biotech Biotechnology Co., Ltd. (HangZhou, China) for transcriptome sequencing. The RNA was initially tested for quantity, purity, and integrity. cDNAoligo(dT) magnetic beads and high-temperature fragmentation technology were subsequently used to capture and fragment mRNAs with a PolyA tail. This was followed by reverse transcription for conversion into cDNA and second-strand synthesis, with a fragment size of approximately 300 bp ± 50 bp, for library construction. Paired-end sequencing was then conducted via an Illumina Novaseq™ 6000 in PE150 mode. The sequencing data underwent quality control procedures, including the removal of adapters and the filtering of low-quality and repetitive sequences. Alignment and transcript assembly were performed via HISAT2 and StringTie software programs. FPKM quantification was carried out via the ballgown package, and significant differences between samples were analysed via the R package edgeR. Genes with a fold change (FC) greater than 2 or less than 0.5 and a p value less than 0.05 were considered differential genes, confirmed by GO and KEGG enrichment analysis.

Bioinformatic analysis

Pancancer RNA expression data were obtained from the TCGA (https://portal.gdc.cancer.gov/) database in three standardized forms: TPM, FPKM, and RPM. OSCC data were extracted from various oral cancer sites within TCGA-HNSC, consisting of 362 OSCC samples and 32 adjacent cancer samples. Clinical information and RNA-seq expression profiles were downloaded for subsequent analysis.

The "limma" package in R (version 4.0.3) was utilized for data integration and analysis, with a focus on differentially expressed genes, through extracting gene names, p values, false discovery rates (FDRs), and

log2-fold change values. Genes with incomplete information were excluded, and those meeting the criteria of FDR < 0.05 and |1log2FC| > 3 were subjected to further analysis. Differential gene visualization was carried out via the "ggplot 2" package. Kaplan–Meier overall survival curves were constructed with the "survial" and "survminer" packages, while ROC analysis was conducted with the "pROC" package, and ROC curves were visualized via "ggplot2". The area under the ROC curve served as an indicator of accuracy in diagnosis and prognosis prediction.

Statistical analysis

Data analysis and statistics were conducted via R and SPSS 23.0. For the data in Table S1, categorical variables (e.g., gender, tumor stage, lymph node metastasis) were compared using the chi-square test or Fisher's exact test, as appropriate. For continuous variables (e.g., age), independent Student's t-tests were used for two-group comparisons. Additionally, Student's t test was utilized to compare two subgroups, whereas one-way ANOVA was used for comparisons among more than two subgroups. Kaplan–Meier survival analysis was conducted to assess the differences in overall survival (OS) based on different YTHDF2 expression levels. A p value less than 0.05 was considered statistically significant.

Results

Upregulated expression of YTHDF2 is correlated with poor prognosis in oral squamous cell carcinoma

To investigate YTHDF2 expression in different cancer types, we analysed the YTHDF2 levels in 33 cancer tissues and compared them to normal tissues. YTHDF2 was found to be upregulated in 13 cancer types, including bladder urothelial carcinoma (BLCA), breast invasive carcinoma (BRCA), cervical squamous cell carcinoma, endocervical adenocarcinoma (CESC), cholangiocarcinoma (CHOL), colon adenocarcinoma (COAD), oesophageal carcinoma (ESCA), glioblastoma multiforme (GBM), head and neck squamous cell carcinoma (HNSC), liver hepatocellular carcinoma (LIHC), lung adenocarcinoma (LUAD), prostate adenocarcinoma (PRAD), stomach adenocarcinoma (STAD), and uterine corpus endometrial carcinoma (UCEC) (Fig. 1A).

In the context of OSCC, significantly higher YTHDF2 expression was observed in OSCC tissues than in normal tissues (Fig. 1B). Higher YTHDF2 expression levels were significantly correlated with advanced tumour grade, as shown in Fig. 1C. OSCC patients were divided into high and low YTHDF2 expression groups on the basis of average YTHDF2 levels, and a Kaplan–Meier curve revealed that the survival time of the high YTHDF2 expression group was significantly lower than that of the low-expression group (Fig. 1D). Furthermore, the diagnostic potential of YTHDF2 expression in OSCC was assessed via receiver operating characteristic (ROC) curve analysis. As shown in Fig. 1E, the area under the curve (AUC) for YTHDF2 was 0.748, with a 95% confidence interval (CI) ranging from 0.664–0.831.

YTHDF2 upregulation was associated with poor prognosis in OSCC

Immunohistochemical staining was conducted on clinical tissue samples to further investigate the correlation between YTHDF2 and the clinical characteristics of OSCC. The results revealed a predominant cytoplasmic expression of YTHDF2 in OSCC tissues through a higher percentage of positive staining and a more intense staining colour (Fig. 2A). Statistical analysis revealed significantly higher YTHDF2 staining scores in OSCC tissues than in control tissues (Fig. 2B). Furthermore, higher levels of YTHDF2 expression were correlated with advanced tumour stage (T_{3+4} and T_{1+2}), advanced clinical stage (C_{III+IV} and C_{I+II}), and lymph node metastasis (L_{N+} vs. $L_{N}-$) (Fig. 2B). K-M analysis revealed a significantly shorter overall survival time in patients with high YTHDF2 expression than in those with low YTHDF2 expression (Fig. 2C). The area under the ROC curve was 0.733 (95% CI 0.626–0.841) (Fig. 2D), indicating that the level of YTHDF2 expression could be a valuable diagnostic marker for OSCC. A staining score cut-off value of 6 was identified for distinguishing OSCC patients from healthy controls.

Knockdown of YTHDF2 suppresses OSCC cell proliferation, migration and invasion

To investigate the impact of YTHDF2 on OSCC cell function, three siRNAs targeting YTHDF2 were synthesized and transfected into SCC9 cells. The knockdown efficiency of these siRNAs in SCC9 cells was determined via RT-PCR and Western blotting (Fig. 3A,B). Among the tested siRNAs, siRNA-1 showed the most effective silencing and was selected for further experiments. Cell proliferation was assessed through CCK-8 and colony formation assays, which revealed that YTHDF2 knockdown significantly inhibited the growth of SCC9 cells (Fig. 3C,D). Additionally, transwell migration and invasion assays indicated that YTHDF2 knockdown resulted in decreased migration and invasion capabilities of SCC9 cells (Fig. 3E,F). The scratch wound assay further confirmed the decreased migration ability of SCC9 cells following YTHDF2 silencing (Fig. 3G,H).

The JAK-STAT pathway may be a potential mechanism for YTHDF2-regulated progression of OSCC

To investigate the potential mechanism underlying the oncogenic role of YTHDF2 in OSCC, we conducted transcriptome sequencing on YTHDF2-silenced cells and control cells. The results revealed a total of 1621 differentially expressed genes in cells after YTHDF2 knockdown, including 740 downregulated genes and 881 upregulated genes (Fig. 4A). Among the thousands of potential targets, STAT1 and STAT2 were significantly upregulated during YTHDF2 knockdown (Fig. 4B). Furthermore, GO analysis of the differentially expressed genes highlighted the critical involvement of YTHDF2 in key processes such as cell proliferation, the inflammatory response, apoptosis, and the immune response in OSCC (Fig. 4C). KEGG analysis further revealed notable alterations in pathways, including the JAK-STAT signalling, Toll-like receptor signalling, NOD-like receptor signalling, P53 signalling, and TNF signalling pathways, following YTHDF2 knockdown (Fig. 4D). Additionally,

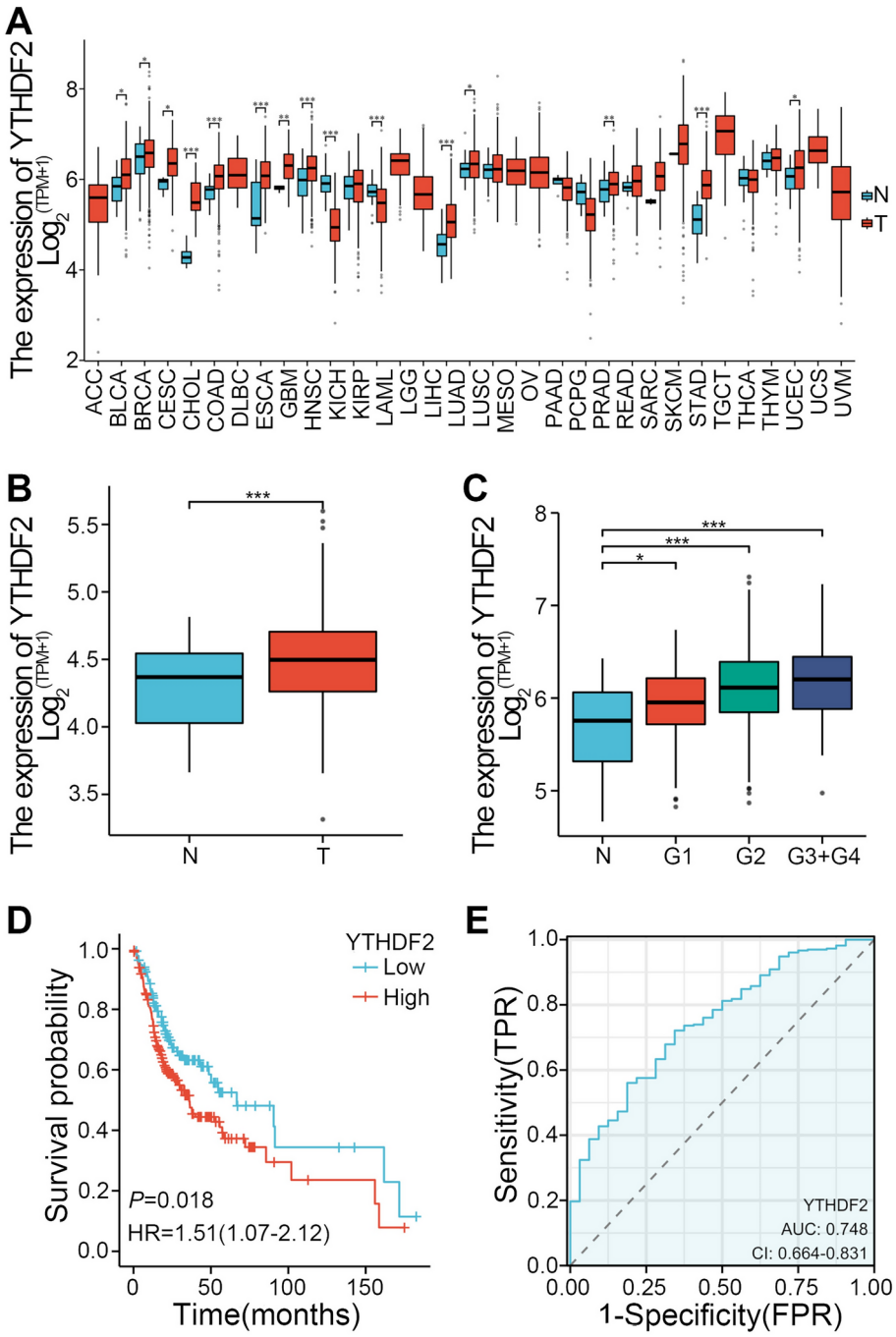

Fig. 1. Upregulated expression of YTHDF2 correlates with poor prognosis in oral squamous cell carcinoma. (**A**) The expression levels of YTHDF2 in various cancers; (**B**) Statistical analysis of YTHDF2 levels in OSCC tissues and normal oral mucosa tissues; (**C**) Statistical analysis of YTHDF2 levels in different clinical grades; (**D**) Kaplan–Meier survival curve based on YTHDF2 expression levels; (**E**) ROC curve analysis of the potential diagnostic value of the YTHDF2 expression level in OSCC diagnosis.

increased expression levels of STAT3 were observed in OSCC tissues compared with normal tissues (Fig. 4E), with a positive correlation between YTHDF2 expression and JAK2 and STAT3 expression (Fig. 4F). These findings suggest that the JAK-STAT signalling pathway could be a potential mechanism by which YTHDF2 regulates OSCC behaviour.

YTHDF2 promoted OSCC growth and metastasis via the JAK-STAT pathway

To confirm that YTHDF2 regulates cell behaviour via the JAK-STAT pathway, we first analysed the protein expression of JAK2 and STAT3 in SCC9 cells after YTHDF2 knockdown. Our results revealed no change in nonphosphorylated JAK2 or STAT3 levels but did reveal a significant decrease in the levels of phosphorylated

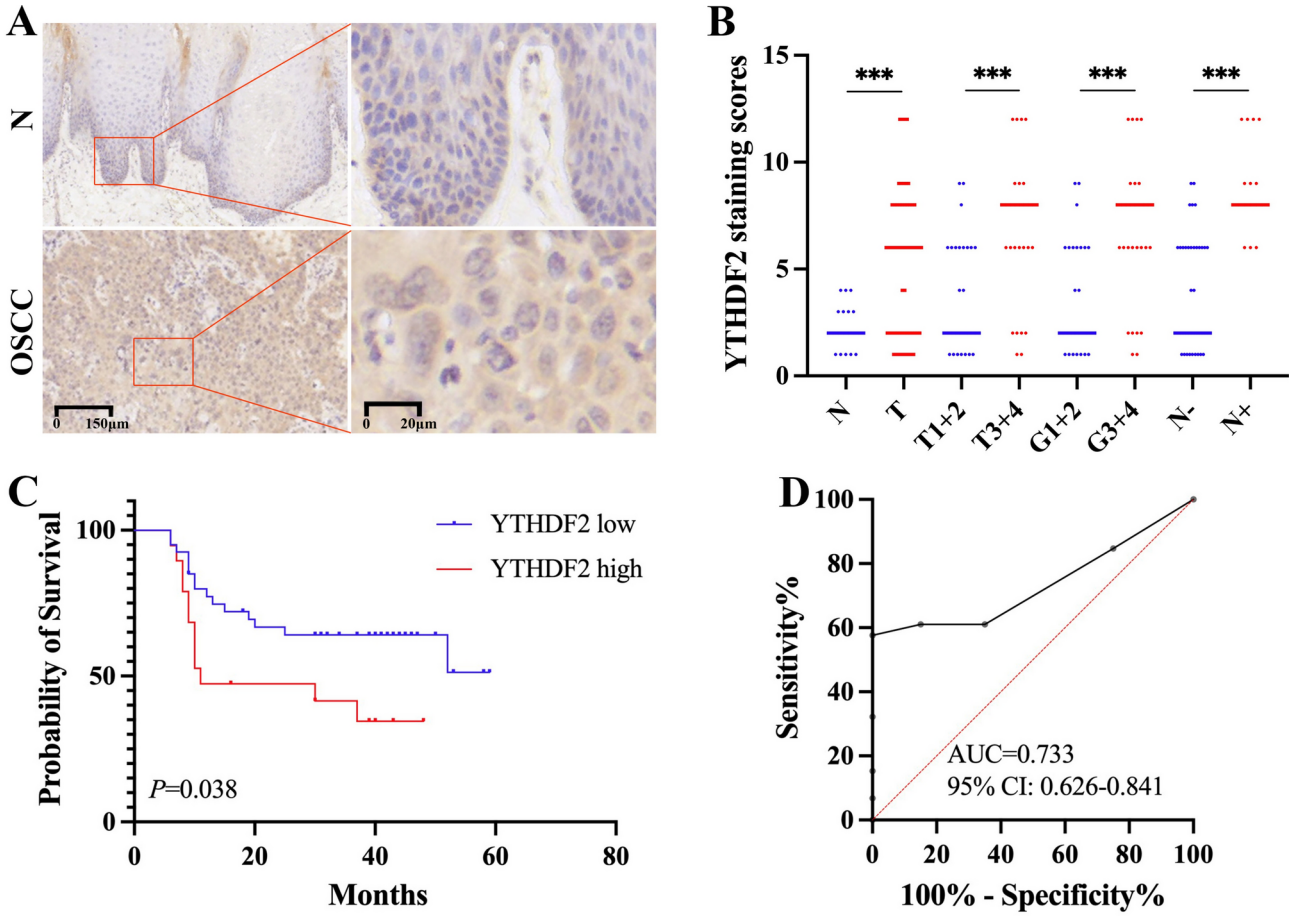

Fig. 2. YTHDF2 was upregulated and associated with poor prognosis in OSCC. (**A**) Results of IHC staining for YTHDF2 in OSCC tissues and paracancerous tissues. (**B**) Statistical analysis of the staining scores of YTHDF2 in OSCC tissues and paracancerous tissues and the relationships between YTHDF2 expression levels and tumour stage (T3 + 4 vs. T1 + 2), clinical stage (CIII + IV vs. CI + II) and lymph node metastasis (LN+ vs. LN−). (**C**) Kaplan–Meier survival curve based on YTHDF2 expression levels. (**D**) ROC curve of the YTHDF2 expression level in OSCC.

JAK2 and STAT3 (Fig. 5A,B). In a rescue experiment, YTHDF2-silenced SCC9 cells were subsequently treated with the STAT3 activator Colivelin. Cell proliferation was assessed via CCK-8 and colony formation assays, whereas cell migration and invasion were analysed via transwell migration, scratch, and invasion assays. As shown in Fig. 5C–H, the cells treated with Colivelin exhibited increased proliferation, migration, and invasion capabilities compared with those in the YTHDF2-silenced group.

Discussion

This study revealed that YTHDF2 is significantly overexpressed in OSCC and is closely associated with the clinical stage, grade, and survival time of OSCC patients. Further investigation into the impact of YTHDF2 on OSCC cell behaviour revealed that downregulation of YTHDF2 led to a decrease in the proliferation, migration, and invasion capabilities of OSCC cells, supporting its role in promoting cancer cell growth and invasion. Transcriptome sequencing results indicated that YTHDF2 may modulate the JAK-STAT signalling pathway. Furthermore, the activation of the JAK-STAT pathway in YTHDF2-knockdown cells partially reversed their reduced proliferation, migration, and invasion abilities. This suggests that YTHDF2 promotes OSCC progression by positively regulating the JAK-STAT signalling pathway.

YTHDF2 primarily regulates mRNA degradation, and its role in various tumours is still debated[17]. While most studies have shown high expression of YTHDF2 in pancreatic cancer[18], liver cancer[19], ovarian cancer[20], cervical cancer[21], where it promotes tumour progression, a minority of scholars have reported a tumour suppressor role for YTHDF2 in certain cancers. For example, Hou et al. [22] reported significant downregulation of YTHDF2 in hepatocellular carcinoma cells, leading to inflammation, vascular abnormalities, and metastasis. Similarly, Shen et al.[23] reported a suppressive function of YTHDF2 in gastric cancer through the destabilization of FOXC2 mRNA. Recent studies further emphasize the context-dependent nature of YTHDF2. For example, YTHDF2 regulates epithelial-mesenchymal transition (EMT) and stemness in bladder cancer via m6A-dependent mechanisms, promoting metastasis[11]. Additionally, YTHDF2 has been reported to stabilize oncogenic mRNAs

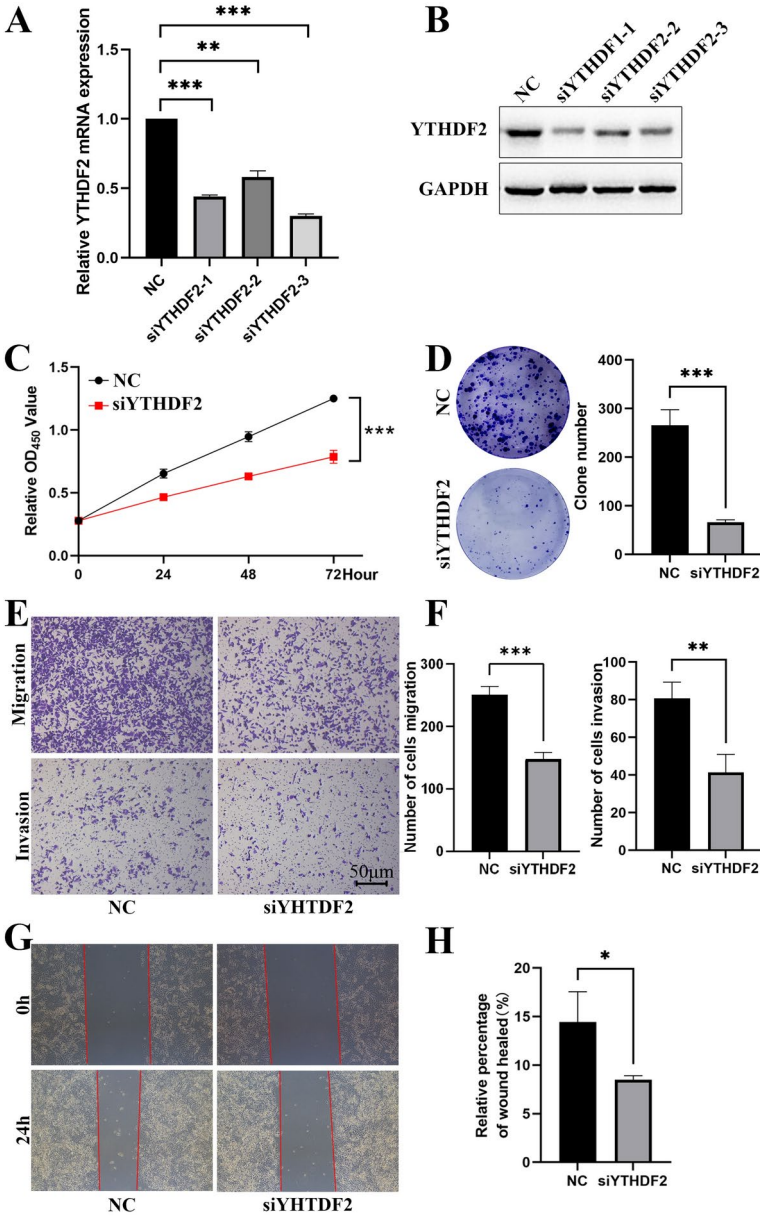

Fig. 3. Knockdown of YTHDF2 suppressed OSCC cell proliferation, migration and invasion. The knockdown of YTHDF2 was confirmed through (**A**) real-time quantitative PCR and (**B**) western blotting. (**C**) CCK-8 detection results, (**D**) colony formation analysis, (**E**,**F**) migration and invasion results, and (G-H) 24-h scratch migration results of the YTHDF2-silenced group and the control group.

in colorectal cancer, further supporting its oncogenic role in specific tumour types[24]. This discrepancy may be attributed to YTHDF2 targeting different mRNAs, including tumour suppressor genes and oncogenes.

The dual roles of YTHDF2 may be influenced by various factors, including tumor type, genetic background, and the tumor microenvironment. For instance, mRNA targets specific to different tumor types could determine whether YTHDF2 functions as an oncogene or a tumor suppressor. In liver cancer, YTHDF2 promotes tumor progression by stabilizing oncogenic transcripts, whereas in gastric cancer, it suppresses tumor growth by destabilizing pro-tumorigenic mRNAs. Moreover, genetic alterations in key pathways may modulate the function of YTHDF2. For instance, mutations in the JAK-STAT signaling pathway or in upstream activators such as IL6R could enhance YTHDF2's oncogenic effects in certain cancers.

However, one limitation of this study is the lack of long-term monitoring or in vivo validation of these findings. Although we have demonstrated the role of YTHDF2 in OSCC progression through in vitro experiments, the physiological relevance and robustness of these results need to be further confirmed in more complex in vivo models. Future research should therefore incorporate xenograft models and long-term monitoring of tumor progression. These approaches would provide more comprehensive insights into the role of YTHDF2 in OSCC and allow for better validation of its potential as a therapeutic target. Additionally, in vivo studies would allow

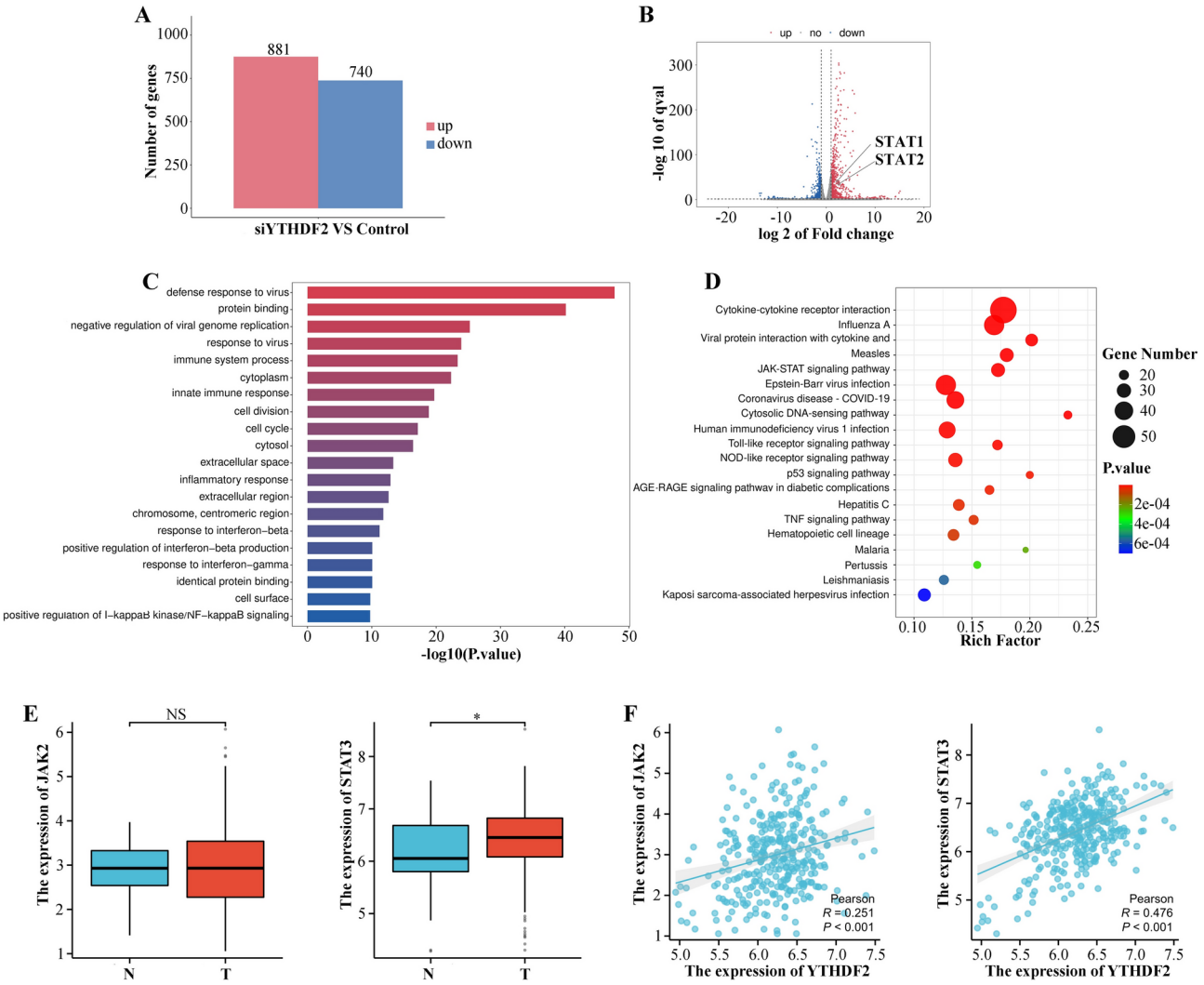

Fig. 4. YTHDF2 regulates the JAK-STAT signalling pathway. (**A**) Statistical analysis of the upregulated or downregulated genes following the knockdown of YTHDF2. (**B**) Volcano plot of the differentially expressed genes after the knockdown of YTHDF2. (**C**) GO and (**D**) KEGG analyses of the possible signalling pathways regulated by YTHDF2. (**E**) JAK2 and STAT3 expression levels in OSCC tissues and normal tissues. (**F**) Correlations between JAK2, STAT3 and YTHDF2 expression in OSCC.

for the exploration of the therapeutic impact of YTHDF2 inhibition in OSCC, which remains an important direction for future investigation.

The tumor microenvironment also plays a critical role in modulating the activity of YTHDF2. Hypoxia, a common feature of the tumor microenvironment, has been shown to upregulate YTHDF2 expression, potentially enhancing its role in promoting metastasis. Similarly, the immune landscape may influence YTHDF2's function by altering its mRNA targets or activity. For example, high levels of immune infiltration may affect the stability and degradation of m6A-modified transcripts regulated by YTHDF2, further contributing to its context-dependent effects.

Although research on YTHDF2 and OSCC is limited, our study revealed that high expression of YTHDF2 in OSCC was correlated with advanced clinical stages, high pathological grades, and short survival times. These results underscore the oncogenic role of YTHDF2 in OSCC and contribute to filling a gap in the current literature.

The JAK-STAT signalling pathway is crucial for regulating various cellular functions, such as proliferation, migration, differentiation, and apoptosis, and plays a significant role in tumour development[25,26]. Activation of this pathway involves JAK initiating tyrosine phosphorylation of receptors thereby recruiting STATs, which form dimers and enter the nucleus to regulate gene transcription[27,28]. Among the STAT family members, STAT3 is particularly important in transmitting signals from the cell membrane to the nucleus[29], and its abnormal expression is associated with multiple cancers, including breast[30], ovarian[31], and lung cancers[32]. Recent studies have further highlighted the role of STAT3 in OSCC, showing that its activation drives stemness, EMT, and therapy resistance in OSCC cells[33]. In particular, the interaction between PD-L1 and STAT3 has been identified as a crucial mechanism promoting immune evasion and metastatic progression in OSCC[14]. Our research

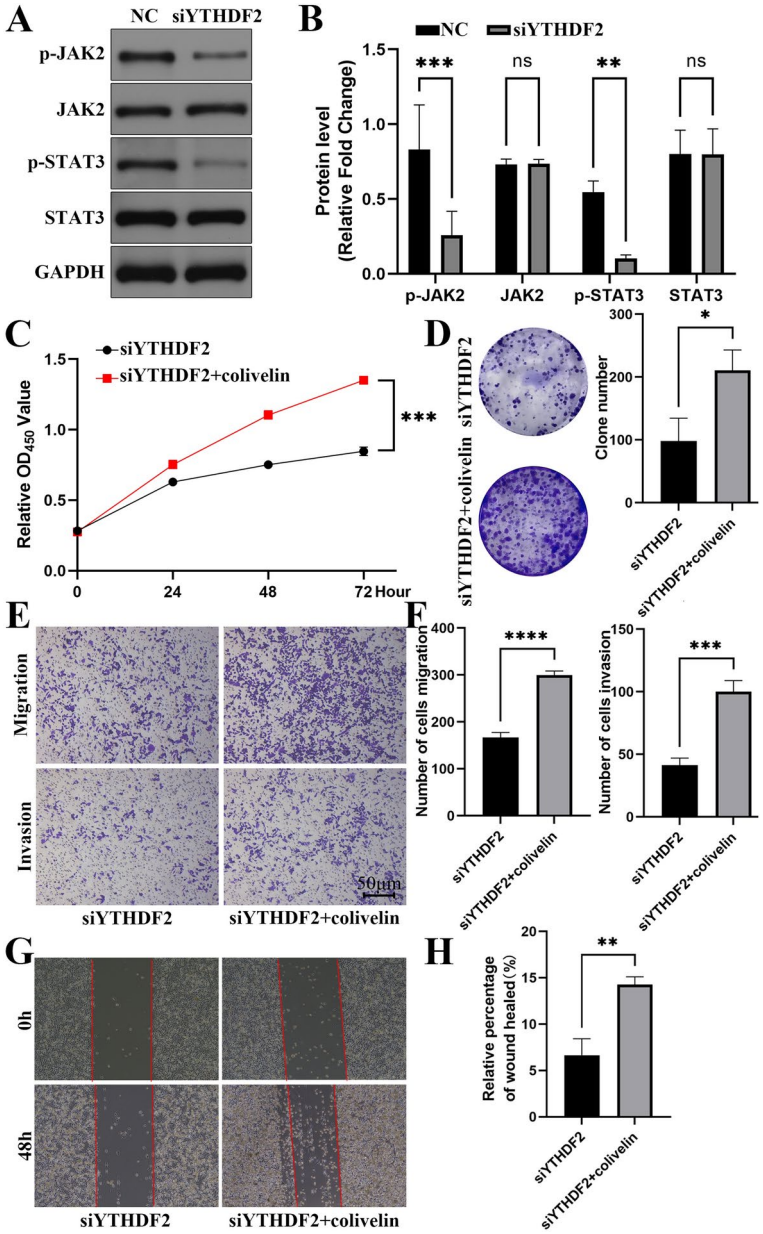

Fig. 5. YTHDF2 promoted OSCC growth and metastasis via the JAK-STAT pathway. (**A**) Expression levels and (**B**) statistical analysis of the JAK and STAT3 proteins between the YTHDF2-silenced group and the control group. (**C**) CCK-8 assay results, (**D**) colony formation analysis, (**E**,**F**) migration and invasion results, and (**G**,**H**) 24-h scratch migration results of the YTHDF2-silenced cells with or without treatment with the STAT3 activator colivelin.

confirmed the high expression of STAT3 in OSCC and revealed the role of YTHDF2 in activating the JAK-STAT pathway to promote OSCC cell malignancy. Despite the tumour-promoting effects of JAK-STAT signalling, some preclinical studies have shown that JAK inhibitors may compromise NK cell antitumour immunity and enhance breast cancer metastasis[34]. In addition, the downstream targets of JAK-STAT signalling in OSCC remain poorly understood and require further investigation.

In future research, we aim to explore the molecular mechanisms linking YTHDF2 with STAT3 activation in OSCC. Recent evidence suggests that YTHDF2 may selectively regulate m6A-modified mRNAs encoding upstream activators of STAT3, such as IL6R and JAK2[35]. Investigating these targets could provide new insights into the crosstalk between m6A modification and STAT3-driven tumor progression. Additionally, the integration of in vivo models and long-term monitoring will be essential to fully validate the role of YTHDF2 in OSCC progression. These findings will contribute to identifying novel therapeutic strategies targeting YTHDF2 or STAT3 in OSCC.

Conclusion

In summary, our study demonstrated the critical function of YTHDF2 in OSCC, which promotes OSCC proliferation and metastasis by regulating the JAK-STAT signalling pathway.

Data availability

The datasets analysed during the current study are available in the TCGA databases repository, (https://portal.gdc.cancer.gov/).

Received: 21 October 2024; Accepted: 27 February 2025
Published online: 21 March 2025

References

1. Hema, K. N., Smitha, T., Sheethal, H. S. & Mirnalini, S. A. Epigenetics in oral squamous cell carcinoma. *J. Oral Maxillofac. Pathol.* **21**(2), 252–259 (2017).
2. Bray, F. et al. Global cancer statistics 2018: GLOBOCAN estimates of incidence and mortality worldwide for 36 cancers in 185 countries. *CA Cancer J. Clin.* **68**(6), 394–424 (2018).
3. Zanoni, D. K. et al. Survival outcomes after treatment of cancer of the oral cavity (1985–2015). *Oral Oncol.* **90**, 115–121 (2019).
4. Almangush, A., Leivo, I. & Mäkitie, A. A. Biomarkers for immunotherapy of oral squamous cell carcinoma: Current status and challenges. *Front. Oncol.* **11**, 616629 (2021).
5. Liu, X. et al. Unraveling the cross-talk between N6-methyladenosine modification and non-coding RNAs in breast cancer: Mechanisms and clinical implications. *Int. J. Cancer.* https://doi.org/10.1002/ijc.34900 (2024).
6. Roundtree, I. A., Evans, M. E., Pan, T. & He, C. Dynamic RNA modifications in gene expression regulation. *Cell* **169**(7), 1187–1200 (2017).
7. Wang, H. et al. RBM15 knockdown impairs the malignancy of cervical cancer by mediating m6A modification of decorin. *Biochem. Genet.* https://doi.org/10.1007/s10528-024-10757-x (2024).
8. Ren, S. et al. Abnormal genetic and epigenetic patterns of m6A regulators associated with tumor microenvironment in colorectal cancer. *Transl. Cancer Res.* **12**(8), 2033–2047 (2023).
9. Paris, J. et al. Targeting the RNA m6A reader YTHDF2 selectively compromises cancer stem cells in acute myeloid leukemia. *Cell Stem Cell.* **25**(1), 137–48.e6 (2019).
10. Zhang, C. et al. YTHDF2 promotes the liver cancer stem cell phenotype and cancer metastasis by regulating OCT4 expression via m6A RNA methylation. *Oncogene.* **39**(23), 4507–4518 (2020).
11. Zhang, L. et al. The m6A reader YTHDF2 promotes bladder cancer progression by suppressing RIG-I-mediated immune response. *Cancer Res.* **83**(11), 1834–1850 (2023).
12. Yang, J. et al. Circular RNA circ_0001105 inhibits progression and metastasis of osteosarcoma by sponging miR-766 and activating YTHDF2 expression. *Onco Targets Ther.* **13**, 1723–1736 (2020).
13. Yang, S. et al. m6A mRNA demethylase FTO regulates melanoma tumorigenicity and response to anti-PD-1 blockade. *Nat. Commun.* **10**(1), 2782 (2019).
14. Jha, A. et al. Crosstalk between PD-L1 and Jak2-Stat3/ MAPK-AP1 signaling promotes oral cancer progression, invasion and therapy resistance. *Int. Immunopharmacol.* **124**(Pt A), 110894 (2023).
15. Yu, M. et al. Bioinformatics analysis of the prognosis and biological significance of N6 methyladenine regulators in oral squamous cell carcinoma. *J. Gene Med.* **26**(1), e3619 (2024).
16. Liu, L. et al. METTL3 promotes tumorigenesis and metastasis through BMI1 m6A methylation in oral squamous cell carcinoma. *Mol. Ther.* **28**(10), 2177–2190 (2020).
17. Du, H. et al. YTHDF2 destabilizes m(6)A-containing RNA through direct recruitment of the CCR4-NOT deadenylase complex. *Nat. Commun.* **7**, 12626 (2016).
18. Chen, J., Sun, Y., Xu, X., Wang, D., He, J., et al. YTH domain family 2 orchestrates epithelial-mesenchymal transition/proliferation dichotomy in pancreatic cancer cells.
19. Nakagawa, N. et al. Novel prognostic implications of YTH domain family 2 in resected hepatocellular carcinoma. *Oncol. Lett.* **22**(1), 538 (2021).
20. Liu, T. et al. The m6A reader YTHDF1 promotes ovarian cancer progression via augmenting EIF3C translation. *Nucleic Acids Res.* **48**(7), 3816–3831 (2020).
21. Wu, M., Chen, G., Liao, X., Xiao, L. & Zheng, J. YTHDF2 interference suppresses the EMT of cervical cancer cells and enhances cisplatin chemosensitivity by regulating AXIN1. *Drug Dev. Res.* **83**(5), 1190–1200 (2022).
22. Hou, J. et al. YTHDF2 reduction fuels inflammation and vascular abnormalization in hepatocellular carcinoma. *Mol. Cancer.* **18**(1), 163 (2019).
23. Shen, X. et al. YTHDF2 inhibits gastric cancer cell growth by regulating FOXC2 signaling pathway. *Front. Genet.* **11**, 592042 (2021).
24. Tang, W. et al. WTAP regulates SOX1 expression to affect the tumorigenicity of colorectal cancer via an m6A-YTHDF2-dependent manner. *Dig. Dis. Sci.* https://doi.org/10.1007/s10620-024-08780-4 (2024).
25. Xue, C. et al. Evolving cognition of the JAK-STAT signaling pathway: autoimmune disorders and cancer. *Signal Transduct. Target Ther.* **8**(1), 204 (2023).
26. Erdogan, F. et al. JAK-STAT core cancer pathway: An integrative cancer interactome analysis. *J. Cell Mol. Med.* **26**(7), 2049–2062 (2022).
27. Xin, P. et al. The role of JAK/STAT signaling pathway and its inhibitors in diseases. *Int. Immunopharmacol.* **80**, 106210 (2020).
28. Puigdevall, L., Michiels, C., Stewardson, C. & Dumoutier, L. JAK/STAT: Why choose a classical or an alternative pathway when you can have both?. *J. Cell Mol. Med.* **26**(7), 1865–1875 (2022).
29. Zou, S. et al. Targeting STAT3 in cancer immunotherapy. *Mol. Cancer.* **19**(1), 145 (2020).
30. Ma, J. H., Qin, L. & Li, X. Role of STAT3 signaling pathway in breast cancer. *Cell Commun. Signal.* **18**(1), 33 (2020).
31. Liang, R. et al. STAT3 signaling in ovarian cancer: A potential therapeutic target. *J. Cancer.* **11**(4), 837–848 (2020).
32. Zhang, X. et al. Hypoxic BMSC-derived exosomal miRNAs promote metastasis of lung cancer cells via STAT3-induced EMT. *Mol. Cancer.* **18**(1), 40 (2019).
33. Zhou, M. et al. Wu Mei Wan suppresses colorectal cancer stemness by regulating Sox9 expression via JAK2/STAT3 pathway. *J. Ethnopharmacol.* **338**(Pt 1), 118998 (2025).
34. Bottos, A. et al. Decreased NK-cell tumour immunosurveillance consequent to JAK inhibition enhances metastasis in breast cancer models. *Nat. Commun.* **7**, 12258 (2016).
35. Yang, Z., Cai, Z., Yang, C., Luo, Z. & Bao, X. ALKBH5 regulates STAT3 activity to affect the proliferation and tumorigenicity of osteosarcoma via an m6A-YTHDF2-dependent manner. *EBioMedicine.* **80**, 104019 (2022).

Reference for citing KEGG images:

36. Kanehisa, M., Furumichi, M., Sato, Y., Matsuura, Y. & Ishiguro-Watanabe, M. KEGG: Biological systems database as a model of the real world. *Nucleic Acids Res.* **53**, D672–D677 (2025).
37. Kanehisa, M. Toward understanding the origin and evolution of cellular organisms. *Protein Sci.* **28**, 1947–1951 (2019).
38. Kanehisa, M. & Goto, S. KEGG: Kyoto Encyclopedia of Genes and Genomes. *Nucleic Acids Res.* **28**, 27–30 (2000).

Acknowledgements
We thank Prof. Anxun Wang (Sun Yat-sen University) for the generous gift of SCC9 and NOK cells.

Author contributions
Z. C. performed the main parts of the experiment; D. Z. analyzed the experimental data and wrote the manuscript; Y. Y., L. Z. and Z. L. provided technical assistance with the experiments; J. C., X. L., Y. H. and L. L. designed and supervised the study. All authors read and approved the final manuscript.

Funding
This work was funded by Luzhou Science and Technology Program (2022-SYF-58), Project of Southwest Medical University (21YYJC0402), Youth Science Climbing Program of The Affiliated Stomatological Hospital of Southwest Medical University (2020QY03) and Sichuan Science and Technology Program (2022YFS0634).

Declarations

Ethics approval and consent to participate
All tissue samples were obtained with the appropriate informed consent and approval from the Institutional Review Board of the Stomatological Hospital Affiliated with Southwest Medical University. We confirm that all experiments were performed in accordance with relevant guidelines and regulations. We also confirm that informed consent was obtained from all participants.

Consent for publication
Not applicable.

Competing interests
The authors declare no competing interests.

Additional information
Supplementary Information The online version contains supplementary material available at https://doi.org/10.1038/s41598-025-92428-4.

Correspondence and requests for materials should be addressed to Y.H. or L.L.

Reprints and permissions information is available at www.nature.com/reprints.

Publisher's note Springer Nature remains neutral with regard to jurisdictional claims in published maps and institutional affiliations.

Open Access This article is licensed under a Creative Commons Attribution-NonCommercial-NoDerivatives 4.0 International License, which permits any non-commercial use, sharing, distribution and reproduction in any medium or format, as long as you give appropriate credit to the original author(s) and the source, provide a link to the Creative Commons licence, and indicate if you modified the licensed material. You do not have permission under this licence to share adapted material derived from this article or parts of it. The images or other third party material in this article are included in the article's Creative Commons licence, unless indicated otherwise in a credit line to the material. If material is not included in the article's Creative Commons licence and your intended use is not permitted by statutory regulation or exceeds the permitted use, you will need to obtain permission directly from the copyright holder. To view a copy of this licence, visit http://creativecommons.org/licenses/by-nc-nd/4.0/.

© The Author(s) 2025